Marine Life Science & Technology (2022) 4:513–526
https://doi.org/10.1007/s42995-022-00146-x

RESEARCH PAPER

Ontogenesis and systematic position of a new hypotrichous ciliate, *Chaetospira sinica* sp. nov., with an improved diagnosis of the poorly defined family Chaetospiridae Jankowski, 1985 (Protozoa, Ciliophora, Hypotrichia)

Wenya Song[1,2] · Xiaotian Luo[3] · Yong Chi[2] · Saleh A. Al-Farraj[4] · Chen Shao[1]

Received: 23 March 2022 / Accepted: 8 September 2022 / Published online: 18 November 2022

Abstract

Ciliates are unique single-celled organisms that play important roles in ecological, environmental, evolutionary, and ontogenetic research. In the present study, phylogenetic analyses based on 18S rRNA gene sequence data reveal that *Chaetospira sinica* sp. nov. clusters with *Stichotricha aculeata* with strong to full support (97% ML, 1.00 BI), but is not closely related to members of Spirofilidae Gelei, 1929 to which *Chaetospira* and *Stichotricha* have previously been assigned. Phylogenetic analyses, together with morphological and morphogenetic data from *Chaetospira sinica* sp. nov., support the validity of family Chaetospiridae Jankowski, 1985. *Chaetospira* and *Stichotricha* are here assigned to the family Chaetospiridae, the improved diagnosis of which is as follows: non-dorsomarginalian Hypotrichia with flask-shaped body; oral region extending along narrow anterior neck region; lorica usually present; two ventral and two marginal cirral rows, all distinctly spiraled or obliquely curved; pretransverse and transverse cirri absent. The basic morphogenetic features in *C. sinica* sp. nov. can be summarized as: (1) the oral primordium for the opisthe develops de novo and the parental adoral zone is completely retained by the proter; (2) all ventral cirral anlagen and marginal anlagen developed intrakinetally; (3) three dorsal kineties anlagen formed intrakinetally in each daughter cell; and (4) macronuclear nodules fuse into a single mass. Exconjugant cells were also isolated and their morphologic and molecular data are provided.

Keywords 18S rRNA gene · Morphogenesis · Phylogeny · Spirofilidae · *Stichotricha*

Introduction

Ciliated protists (Alveolata, Ciliophora) act as important trophic links in the microbial food web of aquatic ecosystems (Bai et al. 2020; Clamp and Lynn 2017; Jung et al. 2021; Liu et al. 2022; Lynn 2008; Omar et al. 2021; Song et al. 2009; Zhang et al. 2022). Hypotrichia Stein, 1859, most of which are dorsoventrally flattened and are substrate-associated or benthic, are considered to be the most complex and highly differentiated ciliate group (Foissner 2016; Kahl 1932; Luo et al. 2021; Park et al. 2020; Vďačný and Foissner 2021). Although hypotrichs have attracted extensive attention, especially in recent years, there are few studies on planktonic representatives of this group (Foissner et al. 1999; Song et al. 2009; Wang et al. 2021b; Zhang et al. 2020). Planktonic hypotrichs have had a confused nomenclatural and taxonomic history because the morphological descriptions of most species are based only on live

Wenya Song, Xiaotian Luo and Yong Chi have contributed equally to this work.

Special topic: Ciliatology.

Edited by Jiamei Li.

✉ Chen Shao
shaochen@snnu.edu.cn

1 Laboratory of Protozoological Biodiversity and Evolution in Wetland, College of Life Sciences, Shaanxi Normal University, Xi'an 710119, China

2 Institute of Evolution & Marine Biodiversity, Ocean University of China, Qingdao 266003, China

3 Key Laboratory of Aquatic Biodiversity and Conservation of Chinese Academy of Sciences, Institute of Hydrobiology, Chinese Academy of Sciences, Wuhan 430072, China

4 Zoology Department, College of Science, King Saud University, Riyadh 11451, Saudi Arabia

observations and lack sufficient characterization by "modern methods". Consequently, the evolutionary relationships within this group remain poorly understood (Corliss 1979; Foissner et al. 1991, 1999; Kahl 1932; Lynn 2008; Ma et al. 2021; Park et al. 2020; Shao et al. 2020).

Chaetospira Lachmann, 1856, a representive member of planktonic hypotrichs, is characterized by its very contractile neck and body, strongly leftward-spiraling marginal and ventral cirral rows and no clearly differentiated frontal or buccal cirrus. Since the genus was established for *Chaetospira muelleri* Lachmann, 1856, another eleven species have been described, almost all based on simple in vivo observations (Dumas 1929, 1937; Kahl 1932). Kahl (1932) and Froud (1949) redescribed the type species, *C. muelleri,* based on in vivo morphology, and the latter author also applied some staining techniques such as Delafield's haematoxylin and the Feulgen reaction. Song and Wilbert (1989) first revealed the infraciliature of *C. muelleri* and improved the diagnosis of the genus. Lynn (2008) classified *Chaetospira* in the family Spirofilidae Gelei, 1929 of the order Stichotrichida. To date, no species of *Chaetospira* has been characterized by morphogenetic and molecular methods.

Due to incomplete morphologic, morphogenetic, and molecular information, the composition and relationships in Stichotrichida are highly inconsistent among several commonly used classification schemes (Corliss 1979; Jankowski 1979, 2007; Lynn 2008; Lynn and Small 2002; Small and Lynn 1985). Consequently, the systematic assignment of *Chaetospira* has been very unstable. Historically, *Chaetospira* has been classified within the families Oxytrichidae Ehrenberg, 1838 (Corliss 1979; Kahl 1932) and Strongylidiidae Fauré-Fremiet 1961 (Corliss 1979). Jankowski in Small and Lynn (1985) established the family Chaetospiridae Jankowski, 1985 for the genus *Chaetospira* with familial diagnostic features as follows: flask-shaped body, transient inhabitation of a lorica, 2 or 3 short ventral rows, no marginal row, oral region extending along narrow, spiral, extensible neck-like anterior region.

Stichotricha, another genus in Stichotrichida, was also assigned to the family Oxytrichidae by Kahl (1932). Jankowski (1979) designated it as the type genus in the subfamily Stichotrichinae but either overlooked or abandoned this in a more recent revision (Jankowski 2007).

In recent classifications by Lynn and Small (2002) and Lynn (2008), both *Chaetospira* and *Stichotricha* were assigned to Spirofilidae (Gelei 1929), a family with *Hypotrichidium* Ilowaisky, 1921 as the type genus. The family Spirofilidae includes taxa with a planktonic lifestyle and has a long history of nomenclatural and taxonomic confusion.

In this study, we describe a new species of *Chaetospira*, *C. sinica* sp. nov., for which we provide morphologic and ontogenetic data for the interphase trophonts and exconjugant cells and details of its 18S rRNA gene sequence. These are the first morphogenetic and gene sequence data for the genus *Chaetospira*. The aims of this work are to: (1) determine the systematic position of *Chaetospira* and assess the validity of the family Chaetospiridae; (2) define the phylogenetic relationship between *Chaetospira* and *Stichotricha*; and (3) improve the diagnosis of the family Chaetospiridae.

Results

Zoobank number for the present work: urn:lsid:zoobank.org:pub:0971F701-0489-4FEE-9913-4A3ABB48E419.

Subclass Hypotrichia Stein, 1859

Family Chaetospiridae Jankowski, 1985

Genus *Chaetospira* Lachmann, 1856

Chaetospira sinica sp. nov.

Zoobank number for the new species: urn:lsid:zoobank.org:act:A52F3D53-667C-408A-85F3-D38EF4AA3B44.

Diagnosis: Body size 100–135×35–50 μm in vivo; body cylindrical in trunk region, with a conspicuously narrow and flexible neck region; contractile vacuole positioned at mid-body; two macronuclear nodules; adoral zone composed of 67–96 adoral membranelles; left and right marginal row with 30–54 and 30–46 cirri, respectively; three dorsal kineties. Freshwater habitat.

Type material: One protargol slide from population I (Id. No. CY2019062601/1) containing the holotype specimen, circled with black ink on the undersurface of the slide (Fig. 1J, K), and seven paratype slides (Id. Nos. CY2019062601/2–8) have been deposited in the Laboratory of Protozoology, Ocean University of China, China. Four paratype slides from population II (Id. Nos. SWY2020081601/1–4, including exconjugants) have also been deposited.

Type locality: A small brook connecting to Lake Weishan wetland (34° 46′ 14″ N, 117° 12′ 56″ E), Shandong Province, China.

Etymology: The specific epithet, *sinica* (L. adjective in nominative singular meaning "Chinese") refers to the place where the new species was discovered.

Description based on population I (Figs. 1A–H, 2A–N, 3A–H; Table 1)

Cell size 100–135×35–50 μm in vivo ($n=7$), ratio of length to width in vivo ranging 2.5–2.9; protargol-stained specimens about 120×56 (range 104–141×41–68) μm, length to width ratio about 2.2:1 (range 1.8–2.7:1). Body broadly obclavate with corkscrew-shaped anterior neck region extending 1/4 of body length, trunk region more or less cylindrical trunk with parallel margins, flexible but contractility not observed (Figs. 1A, D–F, 2A–E, H). Body

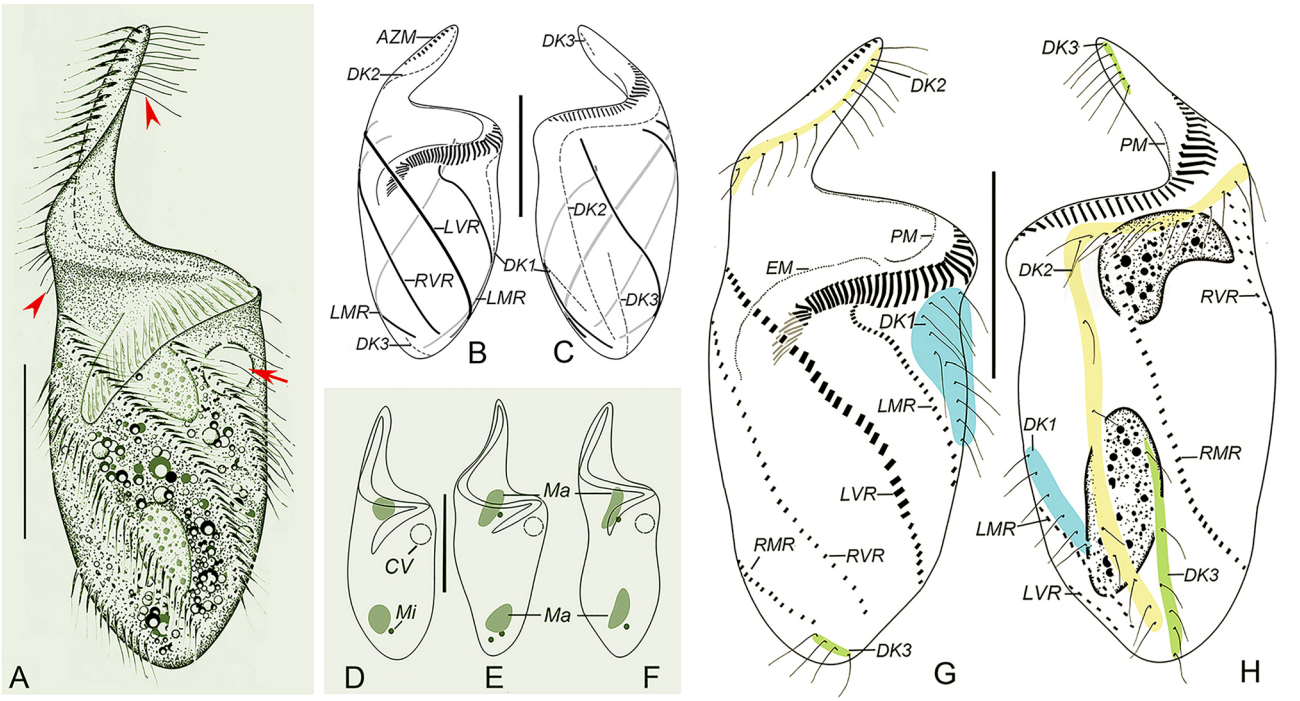

Fig. 1 *Chaetospira sinica* sp. nov. in vivo (**A**, **D–F**) and after protargol staining (**B**, **C**, **G**, **H**) (population I). **A** Ventral view of a representative individual, arrow indicates contractile vacuole, arrowheads show the strikingly long dorsal cilia. **B**, **C** Schematic of ventral and dorsal courses of cirral rows (solid bands) and dorsal kineties (dashed lines). **D–F** Ventral views showing different body shapes and variations in the nuclear apparatus. Ventral (**G**) and dorsal (**H**) view of the holotype, denoting the ciliary pattern and nuclear apparatus. *AZM* adoral zone of membranelles, *CV* contractile vacuole, *DK1–3* dorsal kineties 1–3, *EM* endoral membrane, *LMR* left marginal cirral row, *LVR* left ventral cirral row, *Ma* macronuclear nodules, *Mi* micronuclei, *PM* paroral membrane, *RMR* right marginal cirral row, *RVR* right ventral cirral row. Bars: 30 µm (**A**), 50 µm (**B–H**)

yellow-greenish at low magnification; food particles visible in cells fed with algae (Fig. 2G, I). Cytoplasm colorless, with numerous colorless lipid droplets (Fig. 2M). Cortical granules absent. Invariably two globular to elongate-ellipsoidal macronuclear nodules (15–27 × 8–11 µm in vivo); on average two globular micronuclei (range 1–3) adjacent to macronuclear nodules (Figs. 1A, D–F, H, 2L, 3A, B, H; Table 1). Single contractile vacuole, 8–12 µm across in diastole, located close to left body margin at about midbody, collecting canals not observed (Figs. 1A, D–F, 2B–D). Locomotion by swimming with neck region pointing upwards.

Somatic ciliature comprising four leftward-spiraling cirral rows, i.e., two ventral and two marginal cirral rows, arranged in left-handed spiral around long axis of the body. Each cirrus of marginal and ventral cirral rows comprising two files of basal bodies (Figs. 1A–C, G, H, 3A, B). One left and one right marginal cirral row: left marginal row with 30–54 cirri, commences about cell midline on ventral surface near buccal vertex, terminates on dorsal surface near posterior end of body; right one with 30–46 cirri, begins on dorsal surface near cell midline at level of transverse portion of adoral zone, terminates on ventral surface near posterior end of body (Figs. 1A–C, G, H, 2J, K). Left and right ventral cirral rows consisting of 32–54 and 22–48 cirri, respectively: right ventral row begins on dorsal surface near right cell margin at level of proximal neck region, terminates near posterior end of cell; left ventral row begins slightly dorsally at same level as right ventral row, terminates dorsally near posterior end of cell on left margin. Invariably three dorsal kineties (DK) with strikingly long bristles (11–15 µm in vivo; Figs. 1A, 2F). DK1 composed of 12–20 dikinetids, begins at level of posterior 1/3 of AZM near left body margin, twists onto dorsal side, and terminates in posterior 1/5 of body. DK2 composed of 24–33 dikinetids that are sparsely distributed in midportion, commences at anterior end of body, terminates caudally. DK3 bipartite: anterior part restricted to anterior half of neck region and consists of 6–8 dikinetids; posterior part restricted to posterior 1/2 of trunk region, separated from anterior part by long gap, extends around posterior pole to dorsal side, composed of about 8–12 dikinetids (Figs. 1B, C, G, H, 2F, 3C). Caudal cirri absent.

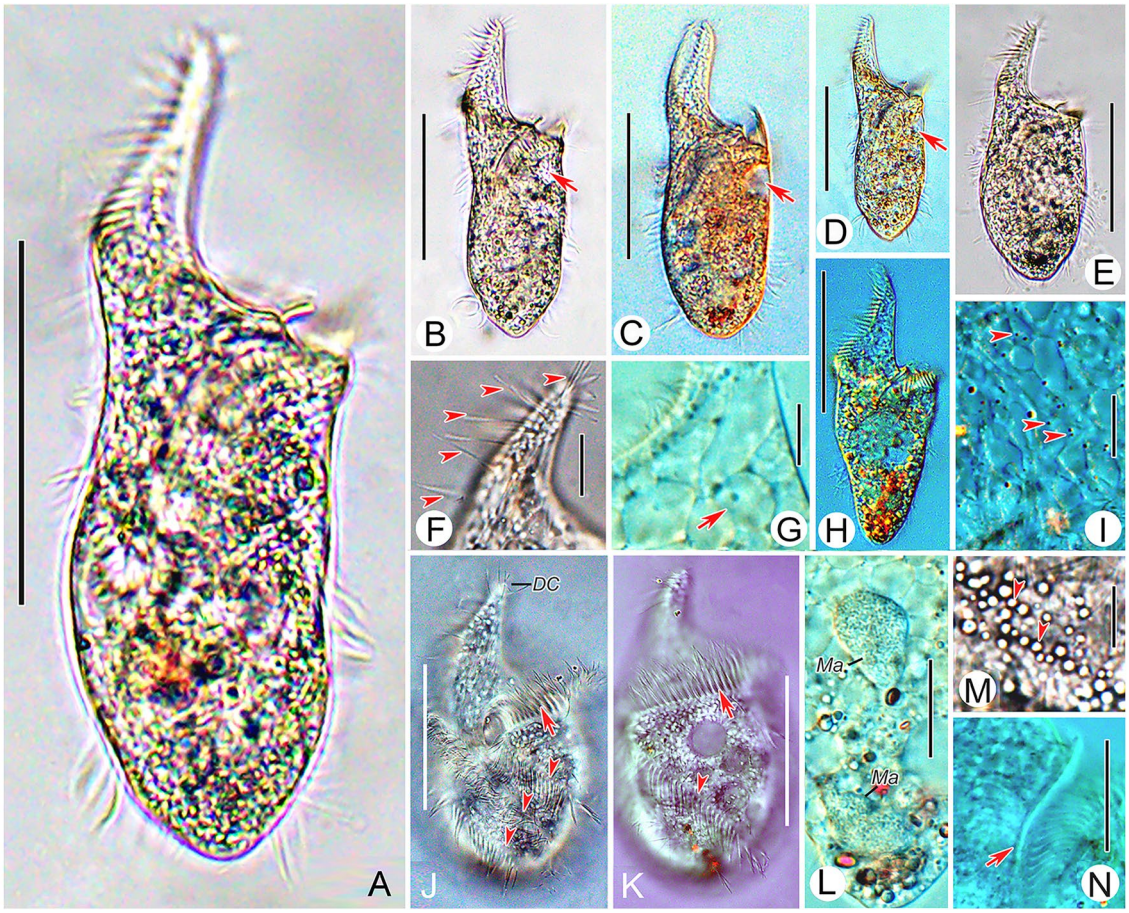

Fig. 2 Photomicrographs of *Chaetospira sinica* sp. nov. from life (population I); **A**, **B**, **E**, **F**, **M** bright field; **C**, **D**, **G–L**, **N** differential interference contrast. **A–E**, **H** Ventral view of a representative cell (**A**) and different individuals **B–E**, **H** arrows in (**B**, **C**, **D**) indicate contractile vacuole. **F** Showing the long dorsal cilia on the neck (arrowheads). Demonstrating the food vacuole (**G**, arrow) and its surrounding particles (**I**, arrowheads). Ventral (**J**) and dorsal (**K**) view, to show adoral zone of membranes (arrows) and cirral rows (arrowheads). **L** Two macronuclear nodules. **M** Lipid droplets (arrowheads). **N** Endoral membrane (arrow). *DC* dorsal cilia, *Ma* macronuclear nodules. Bars: 50 μm

Adoral zone occupies on average 58% of body length (range 46–72%), composed of 84 membranelles on average (range 68–96), commences at anterior end of cell, makes one full spiral turn around neck region, nearly transverse at junction of neck region and trunk, before descending into buccal cavity in anterior 1/3 of trunk region (Figs. 1A–H, 2A–E, H, J, K, 3A, B). Membranelle structure varies from two files of basal bodies in anteriormost part of adoral zone, to three files in middle part of adoral zone, and four files (two very short, nearly equal in length, two very long, also with the same length) in posteriormost part of adoral zone (Fig. 3F, G). Paroral and endoral membranes of nearly equal length, both composed of a single row of ciliated basal bodies; paroral membrane located to right of middle 1/3 of adoral zone, on keel-like elevation at anterior edge of peristome; endoral membrane commences near distal and of paroral membrane, terminates at level of distal end of adoral zone (Figs. 1B, C, G, H, 2N, 3A, D, E).

Morphology of population II (interphase specimens) (Table 1)

The interphase individuals of population II agree well with the population I in all features, except for minor differences in morphometric data after protargol staining (listed in Table 1).

Morphogenesis based on population I (Figs. 4A–I, 5A–M, 6–H)

Stomatogenesis

In the very early stage, the oral primordium of the opisthe develops de novo to the left of the posterior portion of the left ventral cirral row (Figs. 4A, 5A, B). Subsequently, the oral primordium enlarges by further proliferation of basal

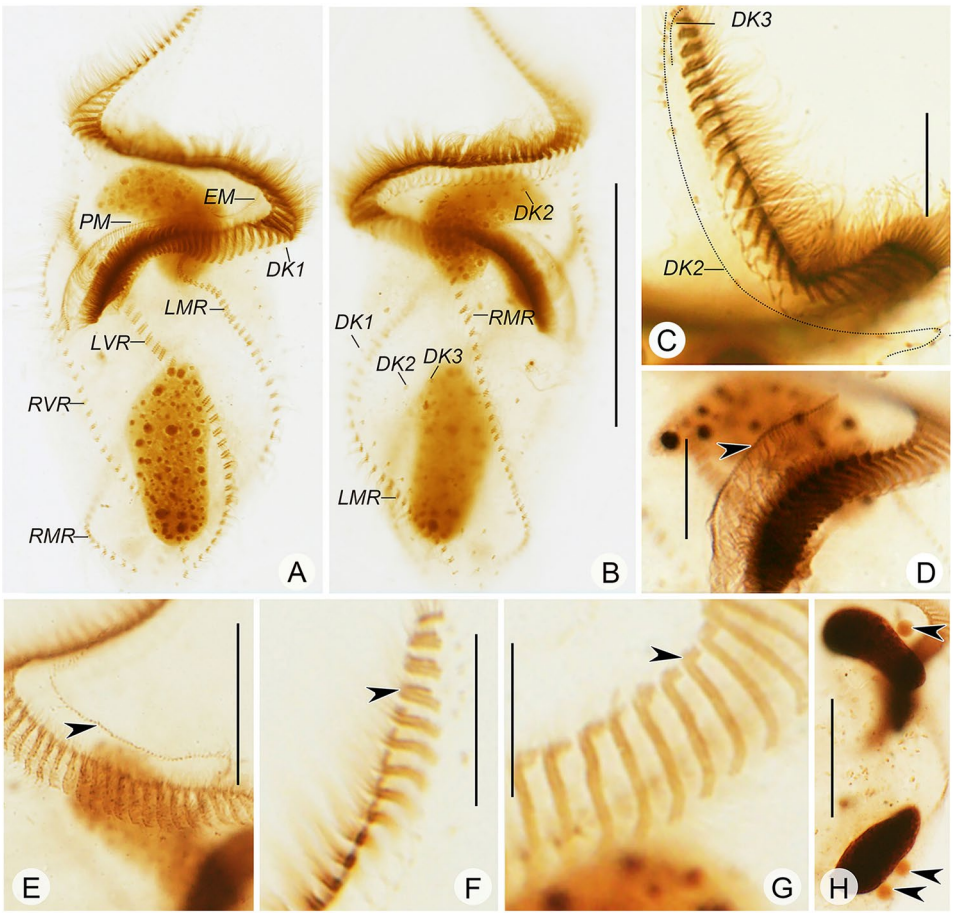

Fig. 3 Infraciliature of *Chaetospira sinica* sp. nov. after protargol staining (population I). **A**, **B** Ventral and dorsal overview of the holotype specimen, to demonstrate the ciliary pattern and nuclear apparatus. **C** Showing dorsal kineties 2 and 3 on the neck region. **D** Denoting the endoral membrane (arrowhead). **E** Arrowhead indicates the paroral membrane. **F** Showing three files of basal bodies in the anterior adoral membranelles. **G** Denoting four files of basal bodies in proximal adoral membranelles. **H** Showing the macronuclear nodules, each with one or two closely associated micronuclei (arrowheads). *DK1–3* dorsal kineties 1–3, *EM* endoral membrane, *LMR* left marginal row, *LVR* left ventral cirral row, *PM* paroral membrane, *RMR* right marginal row, *RVR* right ventral cirral row. Bars: 50 μm (**A**, **B**), 20 μm (**C**, **D**, **H**), 10 μm (**E–G**)

bodies and several membranelles form in the anterior portion (Figs. 4B, C, E, 5C, D). Meanwhile, the undulating membranes anlage (UMA) appears to the right of the oral primordium (Figs. 4B, C, D, 5D). In the proter, the parental paroral begins to disintegrate and forms the UMA for the proter (Fig. 4D–H). From middle to late stages, the formation of the oral primordium for the opisthe is gradually completed from anterior to posterior, and the UMA for each daughter cell splits longitudinally into undulating membranes (Figs. 4H, I, 5K, L, 6A, C, E, G). The parental adoral zone is completely retained by the proter (Figs. 6A–H).

Ventral and marginal cirral rows

In early dividers, the left ventral cirral anlage (LVA) for the proter appears in the anterior part of the old LVR as the parental structure disintegrates (Fig. 4C). Then, the LVA for the opisthe forms in the middle of the parental structure and the right ventral cirral anlage (RVA) for the opisthe develops in the middle of the old right ventral cirral row (Figs. 4D, 5D). Later, the RVA for the proter appears within the old right ventral cirral row (RVR) (Figs. 4F, 5E). Meanwhile, the LVA of the opisthe enlarges to the right of the parental left ventral cirral row (Figs. 4F, G, 5D, E). The left marginal anlage (LMA) for the opisthe and right marginal anlagen (RMA) for proter and opisthe develop intrakinetally (Fig. 4F, G). In the next stage, the LMA for the proter develops within the parental structure (Fig. 4H). Later, all the marginal and ventral cirral anlagen extend bidirectionally (Figs. 4H, I, 5F, G, 6A, B). Finally, the ventral and marginal cirral anlagen begin to differentiate into new cirri for the proter and opisthe and the parental marginal and ventral cirri are resorbed (Figs. 5K, L, 6C–H).

Dorsal ciliature

In early-to-middle dividers, three thread-like dorsal kineties anlagen form intrakinetally in each daughter cell, develop with the proliferation of basal bodies, elongate, and then give rise to DK1–3 (Figs. 4C–I, 5C, I, J, 6A–H).

Nuclear apparatus

In the very early stage, a replication band is present in each macronuclear nodule (Figs. 4C, 5A). The macronuclear apparatus divides in the usual way for hypotrichs, i.e., the

Table 1 Morphometric data of two populations of *Chaetospira sinica* sp. nov

Character	Pop	HT	Min	Max	Mean	M	SD	CV	*n*
Body, length in μm	I	136	104	141	120.1	120.0	8.9	7.4	26
	II	–	101	186	131.8	130.5	16.3	12.4	20
Body, width in μm	I	60	41	68	56.3	56.0	7.2	12.8	26
	II	–	47	76	54.0	51.5	6.2	11.5	20
Body length: width, ratio	I	2.2	1.75	2.67	2.16	2.13	0.25	11.37	26
	II	–	1.70	2.75	2.43	2.48	0.24	9.78	20
AZM, length in μm	I	72	62	80	70.0	68.0	5.1	7.3	26
	II	–	56	83	73.9	76.5	6.6	8.9	20
AZM: body length, ratio	I	0.53	0.46	0.72	0.58	0.59	0.06	10.8	26
	II	–	0.42	0.72	0.57	0.57	0.07	11.5	20
Adoral membranelles, number	I	80	68	96	83.7	86	6.5	7.8	21
	II	–	67	86	76.2	76	5.3	7.0	21
Cirral rows, number	I	4	4	4	4.0	4	0	0	25
	II	–	4	4	4.0	4	0	0	21
Left marginal cirri, number	I	42	30	54	40.6	40	4.9	12.1	25
	II	–	32	46	39.7	41	3.8	9.6	21
Right marginal cirri, number	I	42	30	46	37.9	39	4.5	11.7	25
	II	–	30	43	36.7	37	2.8	7.5	21
Left ventral cirri, number	I	40	32	54	43.0	43	5.4	12.5	25
	II	–	34	51	44.2	45	4.5	10.2	21
Right ventral cirri, number	I	37	22	48	39.1	40	5.9	15.0	25
	II	–	29	47	37.6	38	4.1	10.8	21
Dorsal kineties, number	I	3	3	3	3.0	3	0	0	25
	II	–	3	3	3.0	3	0	0	23
Dikinetids in dorsal kinety 1, number	I	17	12	20	16.4	16	1.9	11.8	25
	II	–	11	20	16.2	16	2.5	15.2	23
Dikinetids in dorsal kinety 2, number	I	33	24	33	27.3	26.0	2.7	9.7	22
	II	–	21	28	25.4	26.0	2.8	11.1	12
Dikinetids in dorsal kinety 3, number	I	16	14	20	16.0	15.5	1.7	10.7	20
	II	–	14	18	15.4	15.0	1.2	7.6	12
Macronuclear nodules, number	I	2	2	2	2.0	2	0	0	25
	II	–	2	2	2.0	2	0	0	25
Micronuclei, number	I	*	1	3	1.8	2	0.5	28.8	25
	II	–	1	2	1.7	2.0	0.5	27.2	20

All data are based on protargol-stained specimens

CV coefficient of variation in %, *HT* holotype, *M* median, *Max* maximum, *Mean* arithmetic mean, *Min* minimum, *n* number of cells measured, *Pop* population, *SD* standard deviation

"*" indicating not observed. Measurements in μm

macronuclear nodules fuse into a single mass during middle stages which then splits twice prior to cytokinesis, and two macronuclear nodules are formed for each daughter cell (Figs. 4E, G, I, 5H, J, M, 6B, D, F, H).

Morphology of exconjugants from population II (Fig. 7A–R)

Body size in vivo 85–110 × 30–40 μm, length to width ratio about 2.8:1 ($n = 6$). Lacriform with anterior end slightly pointed, posterior end rounded (Fig. 7A–E, G, H), highly flexible but contractility not observed. Cytoplasm colorless, containing numerous colorless lipid droplets (0.5–1.0 μm in diameter) (Fig. 7F). Cortical granules not observed. Single contractile vacuole, 11–15 μm across in diastole, located about 40% down length of body near left margin (Fig. 7A–D). Locomotion by swimming at moderate pace while rotating about long axis.

Adoral zone of membranelles straight, occupying about 60% of body length (Fig. 7A–C, I–L). Left marginal cirral row commences 1/3 down length of body and terminates at posterior end of cell. Right marginal cirral row commences at anterior 1/6 of body length and terminates at

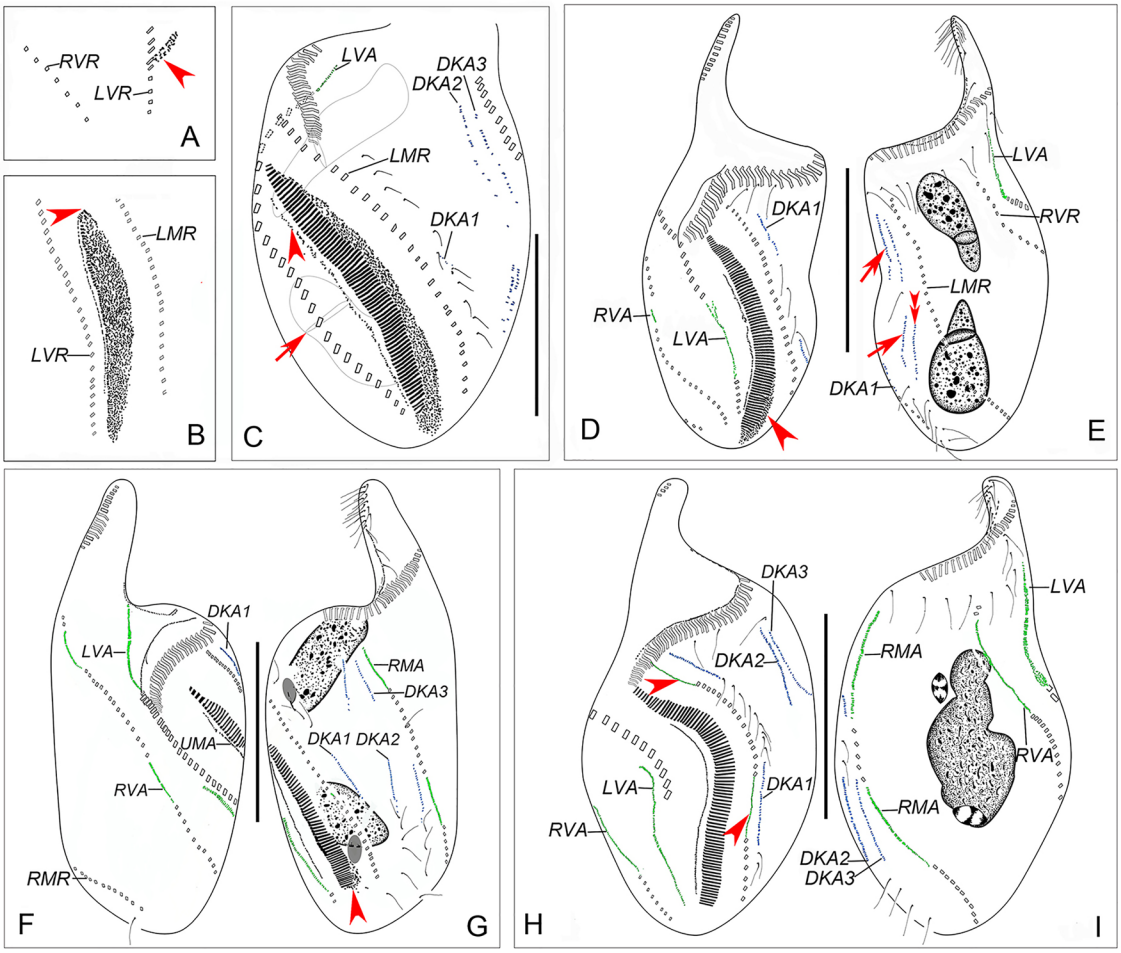

Fig. 4 Early to middle stages of morphogenesis in *Chaetospira sinica* sp. nov. (population I). **A** Ventral view of a very early divider, to demonstrate the oral primordium appearing to the left of the left ventral cirral row (arrowhead). **B** Ventral view of an early divider, to show proliferation of oral primordium basal bodies (arrowhead). **C** Ventral view of an early divider, denoting differentiation of the posterior part of the oral primordium, appearance of the left ventral cirral anlage for proter, and dorsal kineties anlagen. Arrow and arrowhead indicate the undulating membrane anlage and replication band in macronuclear nodule, respectively. Ventral (**D**) and dorsal (**E**) view of the same early divider, arrowhead in (**D**) indicates the differentiating adoral zone of membranelles, arrows and double-arrowhead point to the anlagen of dorsal kineties 2 and 3, respectively. Ventral (**F**) and dorsal (**G**) view of an early-middle divider, to demonstrate the development of the oral primordium and anlagen. Arrowhead in (**G**) marks differentiating adoral zone of membranelles. Ventral (**H**) and dorsal (**I**) view of a middle divider, arrowheads in (**H**) denote the left marginal anlagen. Dorsal kineties and cirral anlagen are shaded blue and green, respectively. *DKA1–3* dorsal kineties anlagen 1–3, *LMR* left marginal row, *LVA* left ventral cirral anlagen, *LVR* left ventral cirral row, *RMA* right marginal anlage, *RMR* right marginal row, *RVA* right ventral cirral anlage, *RVR* right ventral cirral row, *UMA* undulating membrane anlage. Bars: 50 μm

posterior end of cell. Left and right ventral cirral rows commence apically and terminate caudally (Fig. 7A, I–L). Three dorsal kineties with sparsely distributed dikinetids (Fig. 7J, L).

In exconjugants, parental macronuclei fragmented into irregularly ovoidal to long, ribbon-shaped nodules (Fig. 7K–Q). One to three new developing macronuclei observed in different exconjugants (Fig. 7N–R).Whether parental macronuclear fragments fusing with the new developing macronucleus is unknown. No micronucleus was observed in these exconjugants.

18S rRNA gene sequence and phylogenetic analyses (Fig. 8)

The three newly obtained 18S rRNA gene sequences of population I and interphase and exconjugant cells of population II of *Chaetospira sinica* sp. nov. are identical with a length (excluding primers) of 1,667 bp and GC content of 45.89%. They are deposited in the GenBank database with accession numbers, OM313318, OM313319, OM313320, respectively. The most similar sequence to the new species is that of *Stichotricha aculeata* (GenBank number: KR701611) with a sequence similarity of 97.5%, i.e., 41 nucleotide differences.

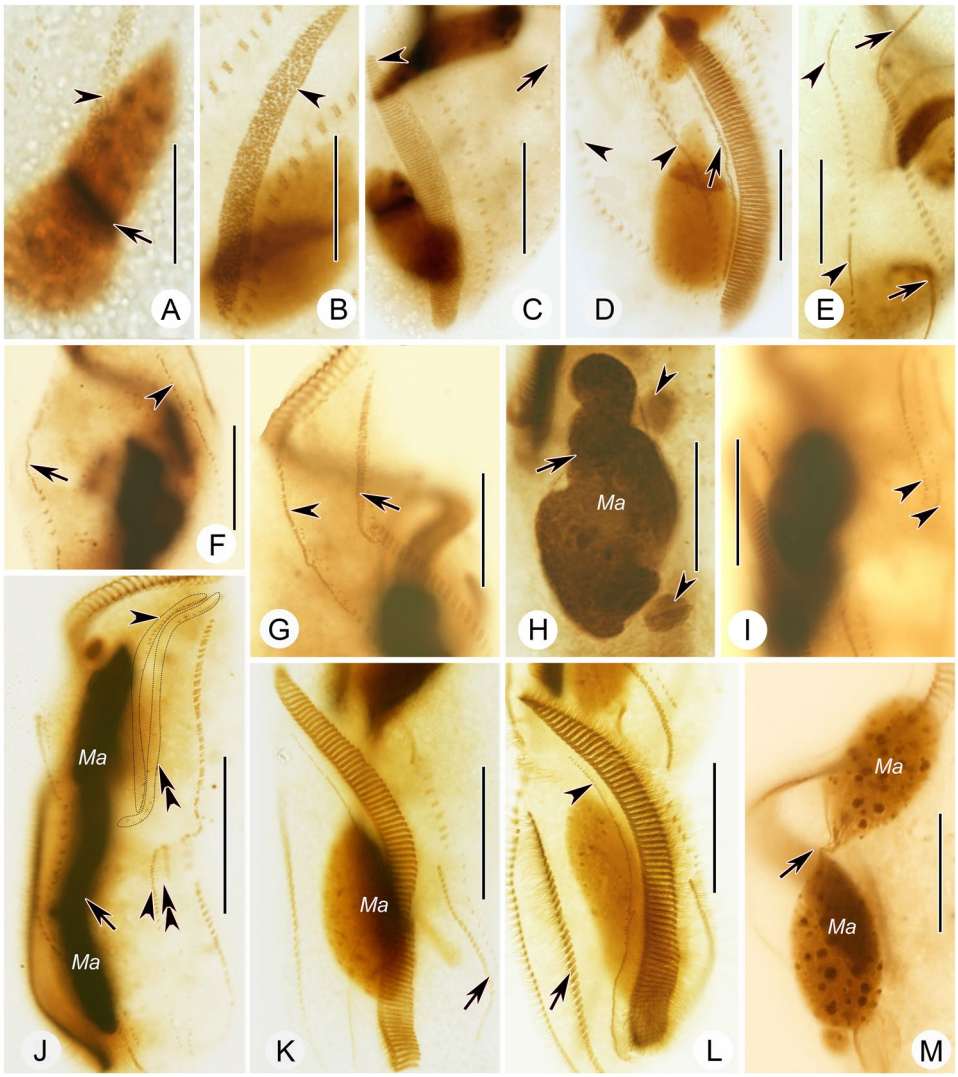

Fig. 5 *Chaetospira sinica* sp. nov. (population I) protargol preparations of cells during morphogenetic process. **A**, **B** Ventral view of very early dividers, to show the oral primordium for the opisthe (arrowheads) and the replication band (arrow). **C** Ventral view of an early divider, demonstrating the newly formed adoral zone of membranelles (arrowhead) and dorsal kinety anlage 2 for the proter (arrow). **D** Ventral view of an early divider, to show the undulating membranes anlage (arrow) and ventral cirral anlagen (arrowheads). Early to middle stages showing the further proliferation of ventral and marginal cirral anlagen, arrows and arrowheads in (**E**, **G**) point to left and right ventral cirral anlagen, respectively; arrow and arrowhead in (**F**) mark left and right marginal anlagen, respectively. **H** Showing the fused macronuclear nodules (arrow) and two micronuclei (arrowheads). **I** Dorsal view of a middle divider, arrowheads mark the dorsal kineties anlagen 2 and 3. **J** Demonstrating the dorsal kinety 2 (arrowheads), dorsal kinety 3 (double-arrowheads), and elongated fused macronuclear nodules (arrow). **K** Ventral view of a late divider, arrow indicates left marginal anlage. **L** A very late divider, arrowhead shows the undulating membranes anlage and arrow points to the left ventral anlage. **M** Arrow points to the splitting macronuclear nodules. *Ma* macronuclear nodules. Bars: 20 μm (**A**), 30 μm (**B–M**)

Phylogenetic trees based on 18S rRNA gene sequence data using Bayesian inference (BI) and maximum likelihood (ML) analyses have almost identical topologies, therefore only the ML tree is shown with nodal support from both methods. The sister relationship between *Chaetospira sinica* and *Stichotricha aculeata* is strongly to fully supported (97% ML, 1.00 BI).

Discussion

Comparison of *Chaetospira sinica* sp. nov. with its congeners

With respect to its body shape, strongly spiralized marginal and ventral cirral rows, and absence of clearly

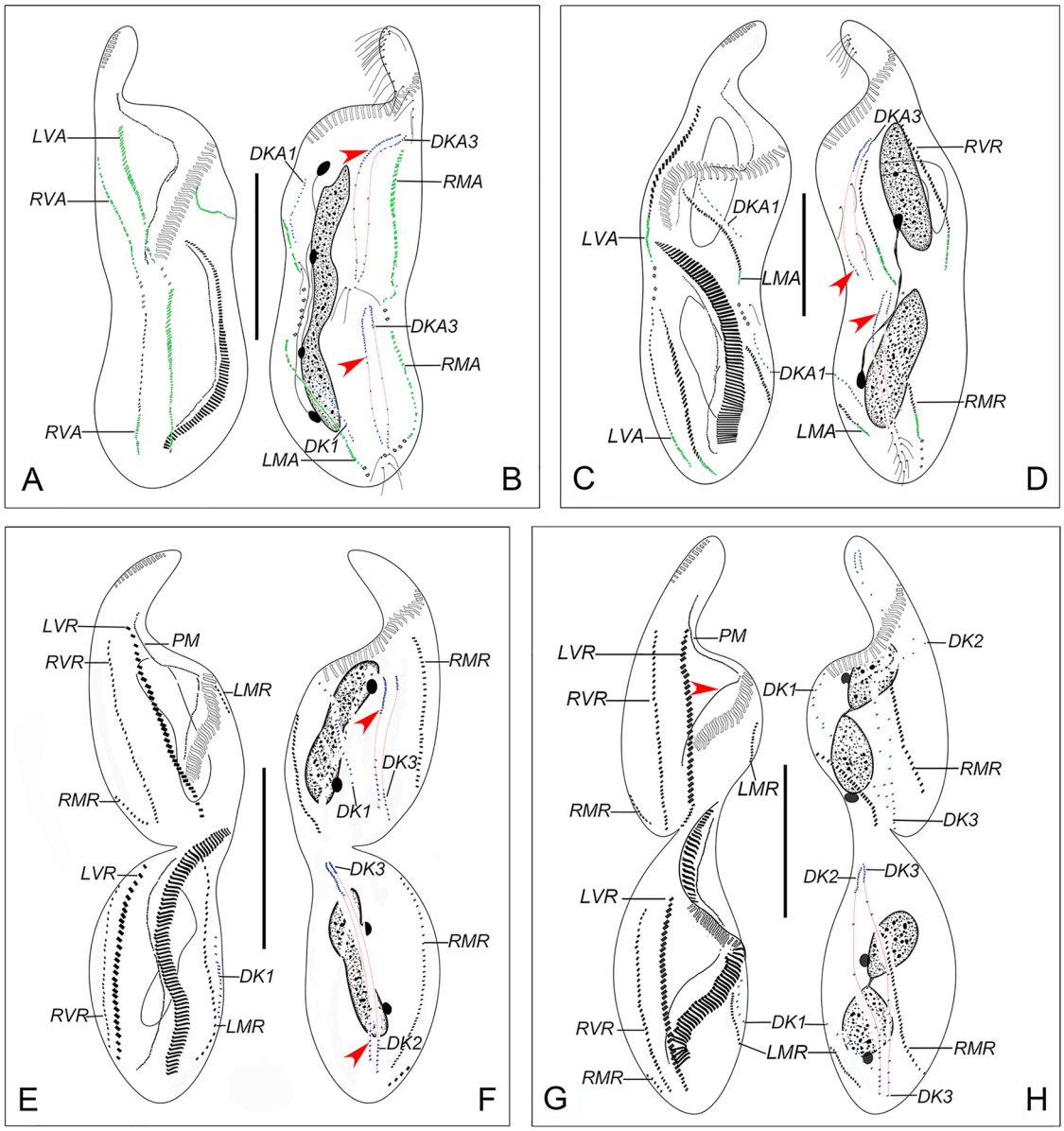

Fig. 6 Middle to late stages of morphogenesis in *Chaetospira sinica* sp. nov. (population I) Ventral (**A**) and dorsal (**B**) view of a middle divider, arrowheads show dorsal kineties anlagen 2. Ventral (**C**) and dorsal (**D**) view of the same late divider, arrowheads point to dorsal kineties anlagen 2. Ventral (**E**) and dorsal (**F**) view of a late divider, arrowheads in (**F**) indicate dorsal kinety 3 in each daughter cell. Ventral (**G**) and dorsal (**H**) view of a very late divider, arrowhead in (**G**) marks endoral membranes in the proter. Dorsal kineties and cirral anlagen are shaded blue and green, respectively. *DK1–3* dorsal kineties 1–3, *DKA1–3* dorsal kineties anlagen 1–3, *LMA* left marginal anlage, *LMR* left marginal row, *LVA* left ventral cirral anlage, *LVR* left cirral row, *PM* paroral membrane, *RMA* right marginal anlage, *RMR* right marginal row, *RVA* right ventral cirral anlage, *RVR* right cirral. Bars: 50 µm

differentiated frontal or buccal cirri, *C. sinica* sp. nov. corresponds well with the diagnostic characteristics of the genus *Chaetospira* given by Song and Wilbert (1989). This may be a non-contractile species but more detailed observations are required to confirm non-contractility as a species character. Furthermore, although all twelve previously described species, i. e., *Chaetospira anguifrons*, *C. congregata*, *C. cornuta*, *C. muelleri*, *C. entzi*, *C. lacrymarioides*, *C. maritima*, *C. monilata, C. mucicola*, *C. remex*, *C. solitaria*, and *C. vaginicola*, are loricate, no lorica was observed in either population of *C. sinica*. The possibility that cells had fled their loricae which were overlooked cannot be completely excluded, but we consider this unlikely.

Additional differences between the new species and its congeners are as follows: *Chaetospira muelleri*, can

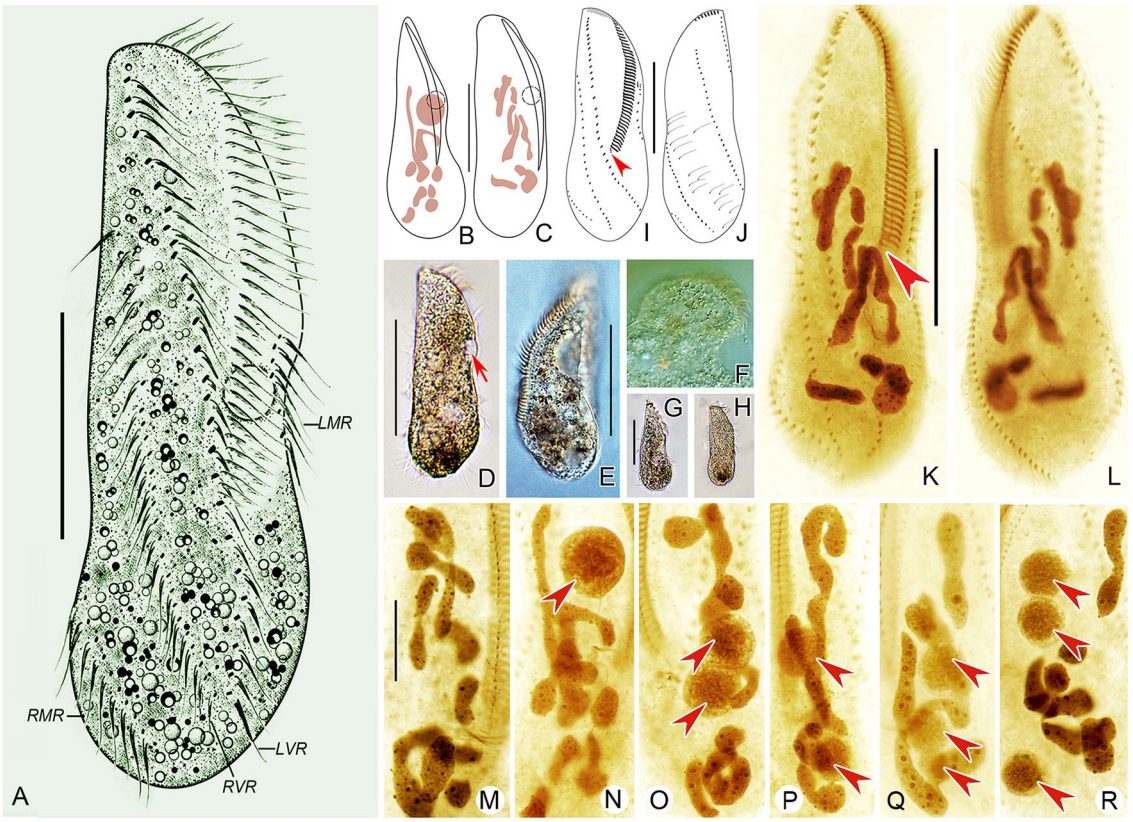

Fig. 7 Exconjugants from life (**A–H**) and after protargol staining (**I–Q**) (population II). **A**, **G** Ventral view. **B**, **C** Ventral views showing different body shapes and macronuclear nodules. **D–H** Ventral (**D**, **G**, **H**) and left lateral (**E**) views of different exconjugants, arrow in (**D**) marks the contractile vacuole. **E** Shows details of the adoral zone. Ventral (**I**) and dorsal (**J**) view of the same exconjugant, showing the infraciliature. Arrowhead in (**I**) indicates incomplete adoral membranes. Ventral (**K**) and dorsal (**L**) view, showing the cirri of an exconjugant, arrowhead in (**K**) indicates the incomplete adoral membranelles. Nuclear events, and formation of new macronucleus (arrowheads in **N–R**). *LMR* left marginal row, *LVR* left ventral cirral row, *RMR* right marginal row, *RVR* right ventral cirral row. Bars: 50 µm

be distinguished from *C. sinica* sp. nov. by having larger body size in vivo (150–300 µm vs. 100–135 µm), a more posteriorly located contractile vacuole (in posterior 1/3 of body vs. in midbody region), shorter dorsal bristles (2 µm vs. 11–15 µm long), and usually four (vs. invariably two) macronuclear nodules (Foissner 1991; Kahl 1932; Song and Wilbert 1989).

Chaetospira entzi was briefly described by Kahl (1932). Although *C. entzi* is similar to *C. sinica* sp. nov. in having two macronuclear nodules, the former can be distinguished from the latter by its more posteriorly located contractile vacuole (posterior 1/3 of cell vs. in midbody region), more slender body, and its longer, more spiralized neck region. Since the number of macronuclear nodules is the same in both species, the possibility that they are conspecific cannot be completely excluded. Further investigation is warranted.

Chaetospira anguifrons, C. cornuta, *C. congregata*, *C. lacrymarioides*, and *C. solitaria* lack detailed morphological descriptions that include information on their ciliature and are characterized only by observations of specimens in vivo. They differ from *C. sinica* sp. nov. by having much more slender body shapes (Dumas 1929).

Chaetospira monilata Jones, 1974 can be distinguished from *C. sinica* sp. nov. by its moniliform macronucleus (vs. two macronuclear nodules) (Jones 1974).

Morphological information for *Chaetospira remex* (Hudson, 1875) Kahl, 1932 is based only on in vivo observations so information on its infraciliature is lacking. *Chaetospira cylindrica* Bolton, 1878 (original combination *Archimedea remex*) is a junior synonym of *C. remex*. The name "*C. cylindracea*" is an incorrect subsequent spelling of *C. cylindrica* (Kent 1882). *Chaetospira remex* differs from *C. sinica* sp. nov. in the shape (slender vs. elongate to ovoid) and length (200–280 µm vs. 100–135 µm) of its body (Foissner 1991; Kahl 1932; Kent 1882).

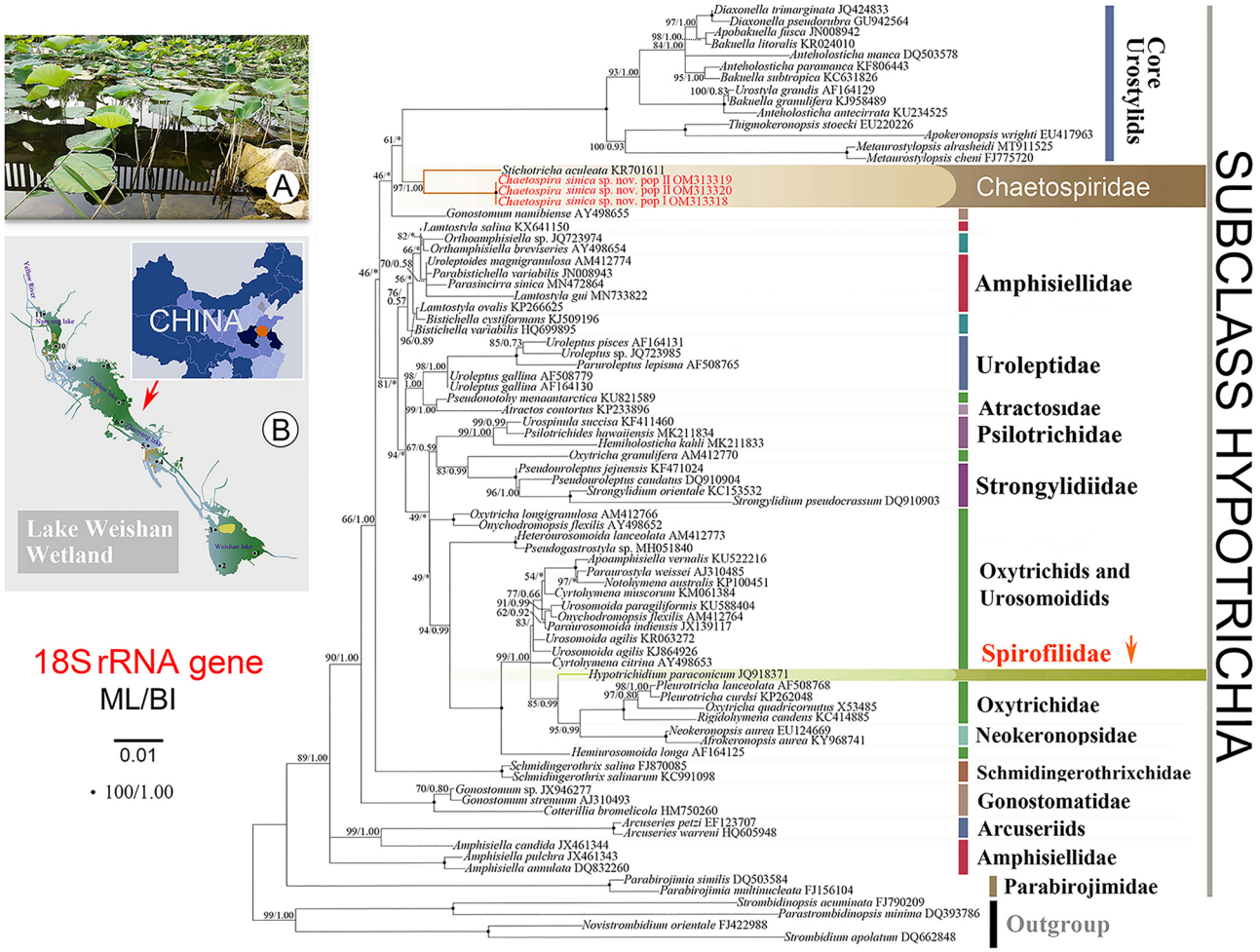

Fig. 8 Maximum likelihood (ML) tree inferred from 18S rRNA gene sequences, showing the systematic position of population I and population II (interphase and exconjugant cell) of *Chaetospira sinica* sp. nov. (indicated in red). **A** The sampling site of population I. **B** The geographic location of the locality. Numbers near branches denote bootstrap values for ML and posterior probabilities for Bayesian inference (BI). Asterisks (*) indicate incongruity between ML and BI trees. Scale bar: one substitution per 100 nucleotide positions

Identification of exconjugants in population II

The morphological data for exconjugants are consistent with the interphase cells in population II. Although interphase and exconjugant cells may differ in body and and in shape, number, and position of macronucleus, their 18S rRNA gene sequences are identical, consistent with conspecificity.

Morphogenetic comparison with similar species

With regard to the spiraling or obliquely curved cirral rows, morphogentic events of four species belonging to three genera, viz. *Atractos contortus* Vörösváry, 1950, *Hypotrichidium conicum* Ilowaisky, 1921, *Hypotrichidium paraconicum* Chen et al., 2013, and *Stichotricha marina* Stein, 1867, have been previously investigated. Each shares certain similar morphogenetic features with *C. sinica* sp. nov., i.e., the parental adoral zone is completely retained by the proter and the oral primordium of the opisthe develops de novo. However, partial cirral anlagen develop de novo in *H. conicum* and *H. paraconicum*, which differs from their intrakinetal generation in *Chaetospira sinica* sp. nov. (Bourland 2015; Chen et al. 2013; Fleury and Fryd-Versavel 1984; Hu and Song 2001; Tuffrau 1970, 1972). Furthermore, morphogenesis in *Atractos contortus* differs from that in *C. sinica* sp. nov. as follows: 1) all marginal and ventral cirral rows develop intrakinetally in *C. sinica* sp. nov., whereas in *A. contortus* the right marginal and ventral cirral rows develop at the posterior ends of the anterior and posterior fragments; and 2) the dorsal kineties anlagen develop intrakinetally in *C. sinica* sp. nov., whereas they develop de novo in *A. contortus* (Bourland 2015).

Familial assignment of *Chaetospira* and *Stichotricha*

The familial assignments of *Chaetospira* and *Stichotricha* have had a complicated history since these genera were established by Lachmann (1856) and Perty (1849), respectively. Kahl (1932) included all non-euplotid hypotrichs, including *Chaetospira* and *Stichotricha*, in the family Oxytrichidae Ehrenberg, 1838. However, the typical frontal-ventral transverse cirral pattern of oxytrichids differs significantly from that in *Chaetospira* and *Stichotricha*, excluding the assignment of these two genera to Oxytrichidae (Berger 1999).

Corliss (1979) placed *Chaetospira* in the family Strongylidiidae Fauré-Fremiet, 1961. However, Strongylidiidae is treated as a junior synonym of Spirofilidae in most recent major revisions (Jankowski 2007; Lynn 2008; Lynn and Small 2002; Shi 1999; Tuffrau and Fleury 1994). Luo et al. (2018), however, reactivated Strongylidiidae for *Strongylidium* Sterki, 1878 (type genus), *Hemiamphisiella* Foissner, 1988 and *Pseudouroleptus* Hemberger, 1985. These three genera differ from *Chaetospira* by having three enlarged frontal cirri, one buccal cirrus, caudal cirri and a mixed formation mode for the long left ventral cirral row, as well as branching distantly from *Chaetospira* in the 18S rRNA gene tree (Fig. 8). Thus, assignment of *Chaetospira* to Strongylidiidae is not supported. Jankowski in Lynn and Small (1985) established the family Chaetospiridae for *Chaetospira*, but this was not accepted in several commonly used systems (Jankowski 2007; Lynn 2008; Lynn and Small 2002).

Jankowski (1979) created the subfamily Stichotrichinae with *Stichotricha* as the type genus but apparently abandoned it in a more recent revision (Jankowski 2007).

In recent systems (Lynn 2008; Lynn and Small 2002), *Chaetospira* and *Stichotricha* were assigned to the Spirofilidae, which was erected for hypotrichs with distinctly spiraled or obliquely curved cirral rows, with *Spirofilum* Gelei, 1929 (junior synonym of *Hypotrichidium*) as the type genus. However, with regard to Spirofilidae, *Chaetospira* and *Stichotricha* differ significantly from the type genus *Hypotrichidium,* e.g., by lacking meridional rows and oblique cirral rows below the buccal vertex (Bourland 2015; Chen et al. 2013; Fleury and Fryd-Versavel 1984; Hu and Song 2001; Tuffrau 1970, 1972). Furthermore, in recent phylogenetic investigations, *H. paraconicum* clustered in the large clade of oxytrichids and neokeronopsids (Chen et al. 2013). These differences argue against the inclusion of *Stichotricha* in Spirofilidae (Bourland 2015; Chen et al. 2013). Borror and Evans (1979) proposed the erection of separate families for the turbinate (i.e., "top-shaped") spirofilids, i.e., *Hypotrichidium*, and the slender tubicolous taxa, i.e., *Stichotricha* and *Chaetospira*, which was accepted by Bourland (2015), but neither Borror and Evans nor Bourland formalized this as a nomenclatural act.

In our molecular phylogenetic analyses, *Chaetospira sinica* sp. nov. is sister to *Stichotricha aculeata* with strong to full support (97% ML, 1.00BI) (Fig. 8). Considering the combination of shared distinctive morphological and morphogenetic features (Bourland 2015; Chen et al. 2013; Hu and Song 2001), together with the phylogenetic analyses, we propose that these two closely related genera share a common ancestor with the following characters: 1) body twisted with four spiral cirral rows; and 2) oral region extending along narrow anterior neck region. Furthermore, *Chaetospira* and *Stichotricha* form a separate clade distant from *Hypotrichidium* and *Strongylidium* (Fig. 8). This indicates that *Chaetospira* and *Stichotricha* do not belong to either Spirofilidae or Strongylidiidae but, instead, represent a distinct family-level taxon.

Hence, the validity of family Chaetospiridae is supported and we assign *Chaetospira* and *Stichotricha* to this family. Jankowski in Small and Lynn (1985), characterized Chaetospiridae as follows: body flask-shaped; cirri only as two or three short ventral rows; marginal cirri absent; oral region extends along narrow, spiral, extensible anterior; lorica present. Since there are two ventral cirral rows and marginal rows are present, an improved diagnosis is provided.

Improved diagnosis for the family Chaetospiridae: Non-dorsomarginalian Hypotrichia with flask- shaped body; oral region extending along narrow, anterior neck region; lorica present in most species; two ventral and two marginal cirral rows, distinctly spiraled or obliquely curved; no pretransverse or transverse cirri.

Type genus: *Chaetospira* Lachmann, 1856.

Genera included: *Chaetospira* Lachmann, 1856, *Stichotricha* Perty, 1849.

Materials and methods

Sample collection, cultivation and identification

Population I of *Chaetospira sinica* sp. nov. was isolated on June 26th 2019 from a small brook that connects with Lake Weishan wetland (Fig. 8A). Population II, including interphase and exconjugant individuals, was collected on August 17th 2020 from an indoor pond. Both sampling sites (34° 46′ 14″ N, 117° 12′ 56″ E) are in the administrative area of Jining, China (Fig. 8B). In each case, a water sample, including sediment, rotting plants, and algae, was transferred to Petri dishes in the laboratory for further processing. A clonal culture for population I was successfully established and maintained for one month at room temperature (about 25 ℃) in Volvic mineral water with 3 µl *Escherichia coli* culture and 20 µl of an algal suspension as food for the ciliates. Raw cultures of population II were established with rice grains added to increase the growth of bacterial food

for the ciliates, but the culture could not be maintained for more than two days.

Cells were observed in vivo according to Wang et al. (2021a) using an Olympus BX53 microscope (Olympus Corporation, Tokyo, Japan). The infraciliature was revealed using the protargol staining method (Wilbert 1975). Measurements were conducted under a light microscope (Zeiss AXIO Imager. D2). Illustrations of individuals during the binary fission process are according to Song and Shao (2017).

DNA extraction, PCR amplification, and sequencing

Genomic DNA was extracted from a single cell from each of population I, the interphase form of population II, and the exconjugant form of population II, according to Ma et al. (2021). The 18S rRNA gene was amplified according to Wu et al. (2020). Q5® Hot Start High-Fidelity DNA Polymerase (New England BioLabs, USA) was used to minimize amplification errors during PCR (Wu et al. 2020). The PCR products were sequenced according to Li et al. (2021).

Molecular phylogeny

A total of 82 sequences were used for phylogenetic analyses, including the three new sequences of *C. sinica* sp. nov. (population I and interphase and exconjugant of population II) and 79 sequences obtained from the National Center for Biotechnology Information (NCBI) database (https://www.ncbi.nlm.nih.gov/) (see Fig. 8 for accession numbers). Four strombidiids were selected as the outgroup taxa. Sequences were aligned by MAFFT (the FFT-NS-1-variant) (Katoh and Standley 2013). The primer sequences were manually trimmed using BioEdit v.7.0 (Hall 1999). The final alignment, comprising 1780 sites, was used to construct phylogenetic trees. Maximum likelihood (ML) and Bayesian inference (BI) analysis were carried out and the tree topologies were visualized according to Wang et al. (2021c).

Acknowledgements This work was financially supported by the National Natural Science Foundation of China (No. 32030015; 32070428; 31900319), the National Key Research and Development Program of China (2018YFD0900701), and the King Saud University, Saudi Arabia (No. RSP2022R7). We would like to express our gratitude to Prof. Helmut Berger (Consulting Engineering Office for Ecology, Salzburg, Austria) for his assistance in providing references from the literature, to Prof. Weibo Song, from Ocean University of China, for his kind help during drafting of the article, to Prof. William Bourland, from Charles University, for his assistance with English, and to the "Weishan Wetland Station" for institutional support.

Authors contributions CS guided the manuscript. WYS and YC carried out the experiments. WYS and XLT finished the molecular phylogenetic analyses and species identification. WYS, XTL, YC, Saleh AA,, and CS drafted the manuscript.

Data availability The datasets presented in this study can be found in online repositories. The names of the repository/repositories and accession numbers can be found below: NCBI (accession: OM313318, OM313319, OM313320); ZooBank (Present work: urn:lsid:zoobank.org:pub:0971F701-0489-4FEE-9913-4A3ABB48E419; *Chaetospira sinica* sp. nov. urn:lsid:zoobank.org:act:A52F3D53-667C-408A-85F3-D38EF4AA3B44)

Declarations

Conflict of interest The authors declare that they have no conflict of interest.

Animal and human rights statements We declare that all applicable international, national, and or institutional guidelines for sampling, care, and experimental use of organisms for the study have been followed and all necessary approvals have been obtained.

References

Bai Y, Wang R, Song W, Suzuki T, Hu X (2020) Redescription of five tintinnine ciliates (Alveolata: Ciliophora: Oligotrichea) from coastal waters of Qingdao, China. Mar Life Sci Technol 2:209–221

Berger H (1999) Monograph of the Oxytrichidae (Ciliophora, Hypotrichia). Monogr Biol 78:1–1080

Borror AC, Evans FR (1979) *Cladotricha* and phylogeny in the suborder Stichotrichina (Ciliophora, Hypotrichida). J Protozool 26:51–55

Bourland WA (2015) Morphology, ontogenesis and molecular characterization of *Atractos contortus* Vörösváry, 1950 and *Stichotricha aculeata* Wrzesniowskiego, 1866 (Ciliophora, Stichotrichida) with consideration of their systematic positions. Eur J Protistol 51:351–373

Chen L, Liu W, Liu A, Al-Rasheid KAS, Shao C (2013) Morphology and molecular phylogeny of a new marine hypotrichous ciliate, *Hypotrichidium paraconicum* n. sp. (Ciliophora, Hypotrichia). J Eukaryot Microbiol 60:588–600

Clamp JC, Lynn DH (2017) Investigating the biodiversity of ciliates in the "Age of Integration." Eur J Protistol 61:314–322

Corliss JO (1979) The Ciliated Protozoa. Characterization, classification and guide to the literature, 2nd edn. Pergamon Press, Oxford

Dumas E (1929) Les microzoaires ou infusoires proprement dits. Faune du centre. 1^{e} fascicule. Les Imprimeries Reunies, Moulins

Dumas E (1937) Les microzoaires ou infusoires proprement dits. Faune du centre. 3^{e} fascicule. Les Imprimeries Reunies, Moulins

Fauré-Fremiet E (1961) Remarques sur la morphologie comparée et la systématique des ciliata Hypotrichida. Académie Des Sciences 252:3515–3519

Fleury A, Fryd-Versavel G (1984) Unité et diversité chez les hypotriches (Protozoaires ciliés) I.—Approche morphogénétique par l'étude de quelques formes peu différenciées. Protistologica 20:525–546

Foissner W (2016) Terrestrial and semiterrestrial ciliates (Protozoa, Ciliophora) from Venezuela and Galápagos. Denisia 35:1–912

Foissner W, Blatterer H, Berger H, Kohmann F (1991) Taxonomische und ökologische Revision der Ciliaten des Saprobiensystems—Band I: Cyrtophorida, Oligotrichida, Hypotrichia, Colpodea. -Informationsberichte des Bayer. Frank, München 1:478

Foissner W, Berger H, Schaumburg J (1999) Identification and ecology of limnetic plankton ciliates. Informationsberichte Des Bayerischen Landesamtes Fur Wasserwirtschaft 3:1–793

Froud J (1949) Observations on hypotrichous ciliates: the genera *Stichotricha* and *Chaetospira*. J Cell Sci 90:141–158
Gelei J (1929) Ein neuer Typ der hypotrichen Infusorien aus der Umgebung von Szeged. *Spirofilum tisiae* n. sp., n. gen., n. fam. Arch Protistenk 80:165–182
Hall TA (1999) BioEdit: a user-friendly biological sequence alignment editor and analyses program for Windows 95/98/NT. Nucleic Acids Symp Ser 41:95–98
Hu X, Song W (2001) Redescription of the little-known marine ciliate, *Stichotricha marina* Stein, 1867 (Ciliophora, Hypotrichida) from the mantle cavity of cultured scallops. Hydrobiologia 464:71–77
Jankowski A (1979) Revision of the order Hypotrichida Stein, 1859. Generic catalogue, phylogeny, taxonomy. Trudy Zool Inst Leningr 86:48–85
Jankowski A (2007) Phylum Ciliophora Doflein, 1901. In: Alimov AF (ed) Protista. Part 2. Handbook on zoology. Russian Academy of Sciences Zoological Institute, St Petersburg
Jones EE (1974) The protozoa of Mobile Bay, Alabama. Univ South Alabama Monogr 1:1–113
Jung JH, Omar A, Park MH, Nguyen TV, Jung YH, Yang HM, Min GS (2021) *Anteholosticha foissneri* n. sp., a marine hypotrich ciliate (Ciliophora: Spirotrichea) from Vietnam: morphology, morphogenesis, and molecular phylogeny. Eur J Protistol 78:125768
Kahl A (1932) Urtiere oder Protozoa I: Wimpertiere oder Ciliata (Infusoria) 3. Spirotricha Tierwelt Dtl 25:399–650
Katoh K, Standley DM (2013) MAFFT multiple sequence alignment software version 7: improvements in performance and usability. Mol Biol Evol 30:772–780
Kent WS (1882) A manual of the infusoria: including a description of all known flagellate, ciliate, and tentaculiferous protozoa, British and foreign, and an account of the organization and affiniities of the sponges. David Bogue, London
Lachmann CFJ (1856) Ueber die Organisation der Infusorien, besonders der Vorticellen. Archiv für Anatomie, Physiologie und wissenschaftliche Medicin, pp 340–398
Li J, Li L, Wang J, Zhu E, Shao C (2021) Morphology, morphogenesis and molecular phylogeny of a novel soil ciliate, *Afrokahliella paramacrostoma* n. sp. (Ciliophora, Hypotrichia). Eur J Protistol 77:125748
Liu M, Liu Y, Zhang T, Lu B, Gao F, Gu J, Al-Farraj SA, Hu X, Song WB (2022) Integrative studies on the taxonomy and molecular phylogeny of four new *Pleuronema* species (Protozoa, Ciliophora, Scuticociliatia). Mar Life Sci Technol 4:179–200
Luo X, Yan Y, Shao C, Al-Farraj SA, Bourland WA, Song W (2018) Morphological, ontogenetic and molecular data support strongylidiids as being closely related to Dorsomarginalia (Protozoa, Ciliophora) and reactivation of the family Strongylidiidae Faure-Fremiet, 1961. Zool J Linn Soc 184:237–254
Luo X, Bourland WA, Song W, Huang J (2021) New contributions to the taxonomy of urostylid ciliates (Ciliophora, Hypotrichia), with establishment of a new genus and new species. Eur J Protistol 80:125810
Lynn DH (2008) The ciliated protozoa: characterization, classification, and guide to the literature, 3rd edn. Springer press, Dordrecht
Lynn DH, Small EB (2002) An illustrated guide to the protozoa. Society of Protozoologists, Lawrence
Ma J, Zhang T, Song W, Shao C (2021) New contributions to the diversity of hypotrichous ciliates: description of a new genus and two new species (Protozoa, Ciliophora). Front Microbiol 12:712269
Omar A, Ji HM, Jung JH (2021) Molecular phylogeny of a new gonostomatid ciliate revealing a discrepancy between interphasic and cell divisional patterns (Ciliophora, Hypotricha). Eur J Protistol 79:125794
Park KM, Jung JH, Kim JH, Min GS, Kim S (2020) Morphology, morphogenesis, and molecular phylogeny of a new freshwater ciliate, *Gonostomum jangbogoensis* n. sp. (Ciliophora, Hypotricha), from Victoria Land. Antarctica. Eur J Protistol 73:125669
Perty M (1849) Mikroskopische Organismen der Alpen und der italienischen Schweiz. Mitt naturf Ges Bern, pp 153–176
Shao C, Chen X, Jiang J (2020) Hypotrichous ciliates in China. Science Press, Beijing
Shi X (1999) Systematic revision of the order Hypotrichida I. Protohypotrichina and Stichotrichina (Ciliophora). Acta Zootaxon Sin 24:241–264
Small EB, Lynn DH (1985) Phylum Ciliophora Doflein. In: Lee JJ, Hutner SH, Bovee EC (eds) An illustrated guide to the Protozoa. Society of Protozoologists, Lawrence, pp 393–575
Song W, Shao C (2017) Ontogenetic patterns of hypotrich ciliates. Science Press, Beijing
Song W, Wilbert N (1989) Taxonomische Untersuchungen an Aufwuchsciliaten (Protozoa, Ciliophora) im Popelsdorfer Weiher, Bonn. Lauterbornia 3:2–221
Song W, Warren A, Hu X (2009) Free-living ciliates in the Bohai and Yellow Seas, China. Science Press, Beijing (**in Chinese**)
Tuffrau M (1970) Nouvelles observations sur l'origine du primordium buccal chez les hypotriches. C R Hebd Séanc Acad Sci, Paris 270:104–107
Tuffrau M (1972) Caractères primitifs et structures évoluées chez les Ciliés hypotriches: le genre *Hypotrichidium*. Protistologica 8:257–266
Tuffrau M, Fleury A (1994) Classe des Hypotrichea Stein, 1859. Traité De Zoologie 2:83–151
Vďačný P, Foissner W (2021) Morphology and ontogenesis of two new *Hemiholosticha* species (Ciliophora, Hypotrichia, Hemiholostichidae nov. fam.). Eur J Protistol 77:125763
Wang J, Zhang T, Li F, Warren A, Li Y, Shao C (2021a) A new hypotrich ciliate, *Oxytricha xianica* sp. nov., with notes on the morphology and phylogeny of a Chinese population of *Oxytricha auripunctata* Blatterer & Foissner, 1988 (Ciliophora, Oxytrichidae). Mar Life Sci Technol 3:303–312
Wang J, Zhao Y, Lu X, Lyu Z, Warren A, Shao C (2021b) Does the *Gonostomum*-patterned oral apparatus in Hypotrichia carry a phylogenetic signal? Evidence from morphological and molecular data based on extended taxon sampling using three nuclear genes (Ciliophora, Spirotrichea). Sci China Life Sci 64:311–322
Wang Z, Wu T, Lu B, Chi Y, Zhang X, Al-Farraj SA, Song W, Warren A, Li L, Wang C (2021c) Integrative studies on a new ciliate *Campanella sinica* n. sp. (Protista, Ciliophora, Peritrichia) based on the morphological and molecular data, with notes on the phylogeny and systematics of the family Epistylididae. Front Microbiol 12:718757
Wilbert N (1975) Eine verbesserte technik der protargolimprägnation für ciliaten. Mikrokosmos 64:171–179
Wu T, Li Y, Lu B, Shen Z, Song W, Warren A (2020) Morphology, taxonomy and molecular phylogeny of three marine peritrich ciliates, including two new species: *Zoothamnium apoarbuscula* n. sp. and *Z. apohentscheli* n. sp. (Protozoa, Ciliophora, Peritrichia). Mar Life Sci Technol 2:334–348
Zhang T, Dong J, Cheng T, Duan L, Shao C (2020) Reconsideration of the taxonomy of the marine ciliate *Neobakuella aenigmatica* Moon et al., 2019 (Protozoa, Ciliophora, Hypotrichia). Mar Life Sci Technol 2:97–108
Zhang X, Lu X, Chi Y, Jiang Y, Wang C, Al-Farraj SA, Vallesi A, Gao F (2022) Timing and characteristics of nuclear events during conjugation and genomic exclusion in *Paramecium multimicronucleatum*. Mar Life Sci Technol 4:317–328